Biochimica et Biophysica Acta 1818 (2012) 2756–2766

Contents lists available at SciVerse ScienceDirect

Biochimica et Biophysica Acta

journal homepage: www.elsevier.com/locate/bbamem

Interfacial behavior and structural properties of a clinical lung surfactant from porcine source

Odalys Blanco [a,b], Antonio Cruz [a], Olga L. Ospina [a,c], Elena López-Rodriguez [a], Luis Vázquez [d], Jesús Pérez-Gil [a,*]

[a] Departamento de Bioquímica, Facultad de Biología, Universidad Complutense, 28040 Madrid, Spain
[b] Centro Nacional de Sanidad Agropecuaria CENSA, San José de las Lajas, Mayabeque, Cuba
[c] Departamento de Fisica, Pontificia Universidad Javeriana, Bogotá, Colombia
[d] Instituto de Ciencia de Materiales de Madrid (CSIC), 28049 Madrid, Spain

ARTICLE INFO

Article history:
Received 10 December 2011
Received in revised form 27 June 2012
Accepted 28 June 2012
Available online 4 July 2012

Keywords:
Pulmonary surfactant
Interfacial film
Surface tension
Epifluorescence microscopy
Calorimetry
Surfacen®

ABSTRACT

Surfacen® is a clinical surfactant preparation of porcine origin, partly depleted of cholesterol, which is widely used in Cuba to treat pre-term babies at risk or already suffering neonatal respiratory distress. In the present study we have characterized the interfacial behavior of Surfacen in several in vitro functional models, including spreading and compression–expansion cycling isotherms in surface balances and in a captive bubble surfactometer, in comparison with the functional properties of whole native surfactant purified from porcine lungs and its reconstituted organic extract, the material from which Surfacen is derived. Surfacen exhibited similar properties to native porcine surfactant or its organic extract to efficiently form stable surface active films at the air–liquid interface, able to consistently reach surface tensions below 5 mN/m upon repetitive compression–expansion cycling. Surfacen films, however, showed a substantially larger and stable compression-driven segregation of condensed lipid phases than exhibited by films formed by native surfactant or its organic extract. In spite of structural differences observed at microscopic level, Surfacen membranes showed a similar thermotropic behavior to membranes from native surfactant or its organic extract, characterized by calorimetry or fluorescence spectroscopy of samples doped with the Laurdan probe. On the other hand, analysis by atomic force microscopy of films formed by Surfacen or by the organic extract of native porcine surfactant revealed a similar network of interconnected condensed nanostructures, suggesting that the organization of the films at the submicroscopic level is the essential feature to support the proper stability and mechanical properties permitting the interfacial surfactant films to facilitate the work of breathing.

1. Introduction

Pulmonary surfactant is a complex mixture of lipids and specific proteins that lines the alveolar epithelium and whose main function is to reduce the surface tension at the air–liquid interface, avoiding the alveolar collapse and reducing the work of breathing [1–3]. The presence of surfactant in the airways is absolutely necessary, being its absence, deficiency or inactivation associated with severe pulmonary diseases [4]. The Infant Respiratory Distress Syndrome (IRDS) is originated by an immaturity of the epithelium to synthesize and secrete a sufficient amount of lung surfactant. In the 80s of the past century, the success of the pioneer therapeutic application of a pharmaceutical preparation of exogenous lung surfactant to treat infants with RDS [5,6] opened a new era in the management and critical care of preterm babies and has contributed to save thousands of lives since then. Different clinical surfactant preparations have been developed and applied to treat babies in the last decades, practically all of them deriving from animal sources, with compositional differences depending on the production method and the variable supplementation with additional lipid components [7]. Comparative studies on the functional behavior of these preparations, in vitro and in vivo, are scarce, and provide a limited correlation with their composition, structure and biophysical properties. Some clinical trials have compared different commercial surfactant preparations, finding relevant differences in clinically-relevant parameters [8,9]. This suggests that a detailed analysis of structure–function correlations of clinical surfactant preparations with respect to fully functional native surfactant can be of interest both to identify and better understand essential features in the surfactant system, and to optimize new strategies in the production of more effective therapeutic surfactants.

Research in the pulmonary surfactant area during the last years has been mainly focused, on the one hand, on attaining a detailed

* Corresponding author at: Departamento de Bioquímica, Facultad de Biología, Universidad Complutense, Jose Antonio Novais 2, 28040 Madrid, Spain. Tel.: +34 913944994; fax: +34 913944672.
E-mail address: jpg@bbm1.ucm.es (J. Pérez-Gil).

0005-2736/$ – see front matter © 2012 Elsevier B.V. All rights reserved.
doi:10.1016/j.bbamem.2012.06.023

description of the molecular interactions and the organization of surfactant structures under functionally relevant conditions [2,10]. On the other hand, pulmonary surfactant research has also pursued the design of simplified surfactant preparations that could allow the substitution of the materials of animal origin, mainly through a proper combination of synthetic lipids and peptides [11].

A major finding was that the particular lipid composition of surfactant is evolutionarily optimized to sustain the segregation in surfactant membranes and films of ordered and disordered phases, which has been related with the particular properties of surfactant in terms of dynamics and mechanical stability [12–16]. Some studies have analyzed to what extent clinical surfactants do capture this structural hallmark of native surfactant and how much the existence of membrane phase segregation could be also associated with proper functional properties [17–19]. In the same line, a recent study has compared in detail the structure of films formed by different clinical surfactants, as seen under atomic force microscopy (AFM) [20]. However, a direct comparison of both the structure and biophysical properties of clinical surfactants with those of their directly related source material is lacking, while it could illustrate how the industrial procedures required to convert an animal-derived material into a clinical product do actually modify its structure and functional behavior.

In the present work, we have evaluated the structure and interfacial properties of films formed by a clinical surfactant preparation of porcine origin, Surfacen®, compared with those of films formed by whole native surfactant purified from porcine lungs or by the organic extract of porcine surfactant once reconstituted in the form of aqueous suspensions.

2. Materials and methods

2.1. Surfactants

Preparations of Surfacen®, a clinical surfactant used in the IRDS therapy in Cuban hospitals [21], were obtained from the Centro Nacional de Sanidad Agropecuaria (CENSA, Mayabeque, Cuba). Surfacen is obtained from organic extracts of porcine bronchoalveolar lavages, which are subjected to acetone precipitation to reduce their content of neutral lipids. It is provided as a sterile white lyophilized powder, dosed in 50 mg phospholipid vials, which still contains the salts of the original saline solution used to obtain the lavage [22]. To reconstitute Surfacen dry powder, the proper amount of the surfactant is therefore weighted and suspended in distilled water, with 60 min preincubation of the suspension at 37 °C, with occasional vortexing, shortly before running functional or structural experiments. Native porcine lung surfactant (NPLS) was obtained from bronchoalveolar lavage of porcine adult fresh lungs obtained from the slaughterhouse, as previously described [23], and stored at −70 °C until its use. The organic extract of native porcine lung surfactant (ENPLS) was obtained by chloroform/methanol extraction of NPLS [24]. To prepare ENPLS aqueous suspensions, the required volume of the extract was first dried under nitrogen and then in UNIVAP for 2 h to remove traces of solvent, and then hydrated in buffer 5 mM Tris pH 7, 150 mM NaCl for 2 h at 45 °C with periodical stirring (1250 rpm every 10 min) in a thermomixer. The different surfactant preparations were quantitated through their phospholipid content, determined using the phosphorus assay described elsewhere [25].

The lipid composition of NPLS, ENPLS and Surfacen was analyzed and compared by thin-layer-chromatography (TLC) in silica gel 60 plates (Merck, Darmstad, Germany), using chloroform:methanol:water (65:25:5,vol/vol/vol) as a mobile phase. Defined amounts of phosphatidylcholine (PC), phosphatidylglycerol (PG), phosphatidylethanolamine (PE), phosphatidylinositol (PI) and cholesterol were applied in the sample plates as reference standards, and the different lipid bands in the TLC plates were visualized under iodine vapors. Selected regions of the TLC plates corresponding to the most important phospholipid components of the surfactant samples were scratched from the plates and subjected to chloroform/methanol extraction, to determine the molar proportion of each of the major phospholipid classes by phosphorus quantitation. The molecular species of the PC fraction of the different surfactant samples were analyzed quantitatively by HPLC coupled to mass spectrometry, with the generous assistance of Drs. Gemma Fabriàs and Josefina Casas, from the Institute of Advanced Chemistry of Catalonia (CSIC) [26].

Analysis of protein content in Surfacen and other surfactant samples was carried out by electrophoresis under reducing conditions. All analyzed samples contained 4.2 μg total phospholipids and were separated in Tris–glycine gels using a Mini-protean IV (Bio-Rad) system. Protein bands were then transferred onto nitrocellulose membranes and analyzed by western blot. For SP-B analysis, membranes were first incubated with SP-B-antibody 1:5000 (rabbit antihuman SP-B, Seven Hills Bioreagents), and then with peroxidase conjugated goat Ig-G anti rabbit (SC-2004 from Santa Cruz Biotechnology). The membranes were subjected to enhanced chemiluminescence assay before exposing them to X-ray films (Immobilon Western, Millipore Corp., Billerica, MA). The same procedure was followed to detect and analyze SP-C content (primary antiSP-C antibody W RAB-MSPC, from Seven Hills Bioreagents).

2.2. Functional assays

2.2.1. Spreading assays in Langmuir surface balances

Suspensions of NPLS, hydrated ENPLS, or Surfacen were applied with a syringe onto the interface of a specially designed T-shaped Teflon trough (15 mL of subphase, buffer 5 mM TRIS pH 7, 150 mM NaCl). The samples are applied in one end of the trough, while a pressure sensor monitors the time-dependent spreading and lateral diffusion of the surface active material arriving at the other end. Spreading isotherms were obtained at 25 and 37 ± 1 °C, upon spreading of different amounts of surfactant (5, 10, 25 or 50 μg total phospholipids).

2.2.2. Pressure–area (π–A) isotherms

π–A isotherms were obtained in a Langmuir surface balance (400 mL buffered saline subphase) equipped with a Teflon ribbon barrier and a Wilhelmy paper plate (NIMA Technology, Coventry, England) [27]. NPLS, hydrated ENPLS or Surfacen suspensions, prepared at 25 mg/mL, were spread dropwise from a syringe at the surface of the balance, and dynamic cycling of the spread film was initiated after a 10 min pause to allow for film equilibration. Isotherms were obtained from ten successive compression–expansion cycles between maximal and minimal trough areas, from 210 to 65 cm^2, at a compression rate of 65 cm^2/min. Temperature was fixed at 25 ± 1 °C, a value at which the large surface of the balance can be stably thermostatized. A large body of precedent data has clearly established that differences in isotherms obtained at 25 °C actually reflect differences in surface behavior of the different materials, which, on the other hand, can be studied under conditions more similar to physiological constraints in the captive bubble surfactometer (see below). The isotherms presented in the figures are representative experiments after at least three repetitions.

2.2.3. Captive bubble surfactometer (CBS)

The surface activity of the different surfactant samples was also evaluated using a fully computer-controlled CBS evolved from the apparatus described earlier [28], operated as described elsewhere [29]. The chamber of the CBS was filled with a buffer solution (5 mM TRIS, 150 mM NaCl, pH 7) containing 10% (by mass) sucrose, to increase the density of the buffer solution (1.04 g/mL) above that of surfactants (~1.01 g/mL). The buffer solution was degassed and a small bubble (50 μL, 3–4 mm diameter) was floated to the ceiling of the sample chamber consisting of a concave agarose gel (1% w/w). The solution was thermostated at 37 °C and left for 10 min to insure 100% humidity of the air bubble. To form the film, 0.2 μL of the surfactant sample (25 mg/mL) was deposited directly at the surface of the

bubble by means of a transparent capillary. The surfactant remained at the air–liquid interface of the bubble due to the density difference with the buffer solution in the chamber. The shape of the bubble was imaged over time by a video camera (Pulnix TM 7 CN) and the video frames were digitized and saved to the computer's hard disk. A first 5-min period following the application of surfactant into the chamber allowed film formation. Changes in surface tension over time were monitored to obtain adsorption kinetics. The chamber was then sealed and the bubble was expanded to a volume of 0.15 mL to monitor post-expansion adsorption. Five minutes after the bubble was expanded, quasi-static cycling commenced, in which the bubble size was first reduced and then enlarged in a stepwise fashion by altering the internal volume of the chamber. Each step had a 3-s change in volume followed by a 4-s delay where the film was allowed to "relax". There was a 1-min delay between each of four quasi-static cycles and a further 1-min delay between the quasi-static and the dynamic cycles. In the dynamic cycles, the bubble size was smoothly varied over the same range as the last quasi-static cycle for 20 cycles at a rate of 20 cycles/min. Bubble volume, interfacial area and surface tension were calculated using height and diameter of the bubble as previously described [30]. Data from initial and post-expansion adsorption are presented as average values from 3 experiments and quasi-static and dynamic cycling isotherms correspond to single representative experiments.

2.2.4. Mechanical stability in CBS

To assess film stability, the films (film coated bubble) were compressed to the minimum possible surface tension without film collapse, then perturbed by a pendulum hammer as previously described [29]. Five perturbations were carried out in succession, as this was judged sufficient in differentiating the samples. This test was carried out in two ways: at the end of the full CBS protocol, i.e. after q-static and dynamic cycling of the films, or immediately after the first quasi-static cycle.

2.3. Structural analysis

2.3.1. Epifluorescence microscopy of surfactant films

Films of NPLS, reconstituted ENPLS, or Surfacen were prepared by spreading the suspensions at 5 mg/mL onto the buffered subphase (0.5 M Tris pH 7 with 0.15 M NaCl) of a modified Langmuir balance (Nima Technology, Coventry, UK), thermostated at 25 ± 1 °C. The suspensions were previously doped with 1 mol percent of the fluorescent lipid [1-palmitoil, 6-(N-7-nitrobenz-2oxa-1,3-diazol-4-il)-PC (NBD-PC), added as an small aliquot of the probe in dimethylsulfoxide (DMSO). Alternatively, monolayers were also prepared from ENPLS or Surfacen extracts (1 mg/mL) in chloroform/methanol (2:1, v/v). After 10 min equilibration, the films were compressed to the required pressure at a compression rate of 25 cm^2/min. After 10 min equilibration, the films were transferred to glass coverslips previously immersed in the subphase, to obtain continuously varying surface pressure (COVASP) films as described previously [31]. This technique allows transfer and characterization of films compressed at different surface pressures, in the same glass support. Epifluorescence images of the supported LB films were acquired in a Zeiss Axioplan II fluorescence microscope (Carl Zeiss, Jena, Germany) equipped with the appropriate fluorescence filters for observation of NBD-PC fluorescence (maximum fluorescence emission at 520 nm).

2.3.2. Atomic force microscopy (AFM) of surfactant films

Samples for AFM were prepared upon transfer of surfactant films onto freshly cleaved mica surfaces using the classic Langmuir–Blodgett method [32]. NPLS or Surfacen monolayers were prepared by spreading organic extract solutions (1 mg/mL) onto the buffer subphase of the surface balance. The films were then compressed until reaching the required surface pressure (37 mN/m) and transferred onto mica supports that were previously immersed in the subphase, while the computer-controlled balance compensates with compression the loss of material to maintain the target pressure constant. The AFM images were obtained with a Multimode Nanoscope IIIA equipped with a type J scanner (Veeco Instruments, Santa Barbara, CA), operated in tapping mode. Tips used were RESTP phosphorus (n) doped silicon probes with a typical radius of less than 10 nm, nominal spring constant of 40 mN/m and resonance frequency between 266 and 309 KHz. Topography and phase images were recorded from each sample with 512 scan lines and a frame rate of 0.5 Hz.

2.3.3. Calorimetry

The analysis of the thermotropic properties of surfactant samples was carried out by differential scanning calorimetry (DSC) of the samples in a VP-DSC MicroCal calorimeter (Baltimore, MD). The sample cells were loaded with 0.5 mL of 5 mg/mL of NPLS, ENPLS or Surfacen suspensions, while the reference cell was loaded with an equivalent aliquot of buffer. Ten consecutive scans were obtained over a temperature from 5 to 60 °C at a scan rate of 30 °C/h. The resulting thermograms were processed to subtract the baseline and to estimate the enthalpy associated and the transition temperature (Tm) of the main transitions using the Origin Software (Northampton, MA). The DSC curves presented in the figures are representative of at least three different experiments.

2.3.4. LAURDAN fluorescence

Thermotropic phase transitions in NPLS, ENPLS and Surfacen suspensions were also characterized by following the temperature-dependent shift of the fluorescence of a trace (1% with respect to phospholipid, mol/mol) of the fluorescent probe LAURDAN, as previously described [33]. LAURDAN was incorporated into surfactant samples as a small dimethylsulfoxide aliquot, and the final phospholipid concentration was of 10 μg/mL. The fluorescence spectra of all samples were recorded in an Aminco-Bowman Series 2 luminescence spectrometer equipped with thermostated cells, using an excitation wavelength of 370 nm and recording the emission between 400 and 550 nm, within a temperature range of 10 to 60 °C. The results were expressed as a generalized polarization function (GPF), defined as $GPF = (I_B - I_R)/I_B - I_R$ being I_B and I_R the intensities at the blue and red edges of the emission spectrum, respectively [33,34].

2.4. Data reproducibility and statistics

When possible, the figures represent the mean ± S.D. after averaging data from three independent experiments, with at least two different batches of each surfactant material. Langmuir and CBS compression–expansion experiments are illustrated as representative isotherms of each type of surfactant material. Statistical significance of differences in composition or surface behavior was analyzed using one way analysis of variance (ANOVA). Particularly, Holm–Sidak method was applied for multiple comparison versus control group, with significance level = 0.05. To compare two particular groups the Mann–Whitney Rank Sum Test was applied.

3. Results

3.1. Lipid and protein composition of surfactant preparations

Fig. 1 illustrates a comparative compositional analysis of the lipid fraction in NPLS, ENPLS and Surfacen preparations. The three materials contain more than 90% by weight of phospholipids, being phosphatidylcholine (PC) the main phospholipid class, which accounts for 79.5 ± 1, 81.9 ± 0.3 and 74.1 ± 2.1% of phospholipid mass in NPLS, ENPLS and Surfacen, respectively. The main anionic phospholipid in our NPLS and ENPLS preparations is phosphatidylinositol (PI), whilst phosphatidylglycerol (PG) is the main negatively charged phospholipid

in Surfacen. Our so-termed "PG fraction" may also include a minor amount of PE that is not resolved in the TLC system used. However, we know from previous studies that PE is a very minor phospholipid class in these preparations. All the batches analyzed of the three surfactant preparations contained similar proportions of PI, in the order of 10–15%, being the proportion of PG that showing the largest differences. NPLS and ENPLS batches always contained significantly lower amounts of PG, in the order of 4–8%, than Surfacen, which contained 12–16% PG. The analysis of phospholipid molecular species in the PC fraction of the three surfactant samples revealed that dipalmitoylphosphatidylcholine (16:0/16:0, DPPC) was always the main species, accounting for around 70% of PC in NPLS and ENPLS and up to 78–80% of PC in Surfacen. Interestingly, the proportion of other disaturated PC species, palmitoylmiristoyl-PC (16:0/14:0, PMPC), was lower in Surfacen (~9%) than in NPSL and ENPSL (11–14%). The lower proportion of PMPC with increased amounts of DPPC possibly reflects compositional differences in the source material of Surfacen with respect to that of our NPLS and ENPLS preparations, likely as a consequence of differences in animal strains, nutrition and other environmental variables, as it has been reported [35]. The TLC in Fig. 1 also illustrates a major difference in the lipid composition of Surfacen compared to NPLS and ENPLS. Production of Surfacen involves an acetone precipitation step, which reduces significantly the content of cholesterol, from $3.2 \pm 0.2\%$ to $0.8 \pm 0.2\%$ with respect to phospholipid by mass.

On the other hand, Fig. 2 shows illustrative western blots comparing the relative content of proteins SP-B and SP-C in the different samples studied. Surfacen contains well-detectable proportions of both proteins, in the order of 0.7% SP-C and 0.4% SP-B with respect to phospholipid by mass, comparable in broad terms to the amounts of SP-B and SP-C present in a well known clinical surfactant like Curosurf (samples generously provided by Prof. Adolf Valls, from Hospital Cruces, Bilbao, Spain).

3.2. Interfacial properties of surfactant films

Fig. 3 compares π–t spreading kinetics of suspensions of NPLS, ENPLS and Surfacen at the interface, at 25 and 37 °C. The three surfactant materials adsorb very efficiently at the interface at 37 °C, producing equilibrium surface pressures of around 43 mN/m in less than a minute. The amount of material required to reach maximal pressure somehow differs in the different samples. Ten microgram of NPLS is enough to form a film at maximal pressure, while at least 25 μg is required for ENPLS or Surfacen to reach similar equilibrium values. Differences in spreading capabilities were maximized when the different materials were tested at 25 °C. The whole native NPLS material showed significantly better adsorption properties than ENPLS or Surfacen, which behaved very similarly. Maximal pressures reached by Surfacen upon adsorption at either 25 °C or 37 °C were indistinguishable from those reached by ENPLS, but significantly lower than pressures produced by equivalent amounts of NPLS ($p<0.05$).

To analyze the ability of interfacial films formed by adsorption of the three compared materials to reach very low surface tension (high surface pressure) under compression, we run compression–expansion cycling isotherms in a Langmuir surface balance (see Fig. 4), at 25 °C. All the films exhibited qualitatively similar isotherms, with long exclusion (compression) and reinsertion (expansion) plateaus, reaching surface pressures above 70 mN/m upon cyclic compression. None of the films reached pressures of 70 mN/m during the first compression cycle, although films formed by spreading of whole NPLS produced significantly higher pressures than ENPLS or Surfacen films ($p<0.05$). Remarkably, the successive compression–expansion cycles improved progressively the properties of the three materials, which consistently reached maximal pressures from the third compression cycle, as it can be observed in the insets of Fig. 4. The films of NPLS, ENPLS or Surfacen were very stable, as they maintained minimal pressures above 25 mN/m during all the cycles. In this respect, films formed by Surfacen maintained significantly higher minimal pressures ($p<0.05$) than films made by ENPLS.

To compare the biophysical behavior of the surfactant materials under more physiologically relevant conditions of high surfactant concentrations and physiological temperature, Fig. 5 summarizes adsorption and quasi-static and dynamic cycling isotherms obtained in a captive bubble surfactometer. The three materials, NPLS, ENPLS and Surfacen, showed absolutely comparable initial adsorption properties

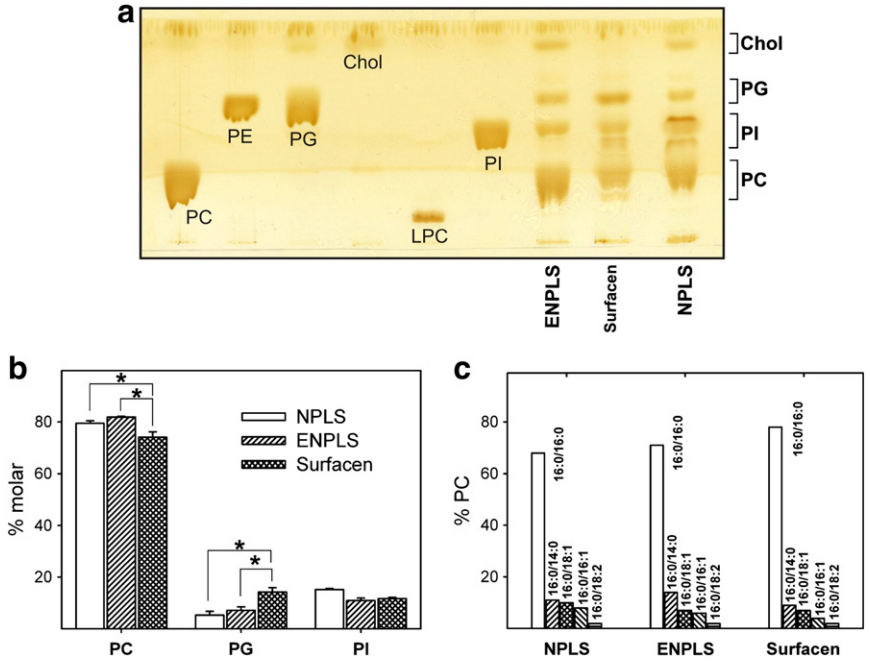

Fig. 1. Compositional analysis of the lipid fraction of native surfactant and Surfacen. a) Thin-layer-chromatographic (TLC) analysis of the lipid composition of NPLS, ENPLS and Surfacen. 100 μg of total phospholipid were applied from each sample in the TLC plate and developed using chloroform/methanol/water (65:25:5, v/v/v) as elution system. Hundred micrograms of each of the indicated standard lipid classes was applied in the same TLC plate as a reference. b) Quantitative compositional profile of the main phospholipid classes in NPLS, ENPLS and Surfacen as determined by phosphorus quantitation of each of the TLC bands in the regions defined in the chromatogram. The asterisk indicates statistically significant differences ($p<0.05$). c) Quantitative compositional profile of molecular species in the PC fraction of a representative batch of NPLS, ENPLS and Surfacen, determined by mass spectrometry lipidomic analysis of the PC band obtained from TLC.

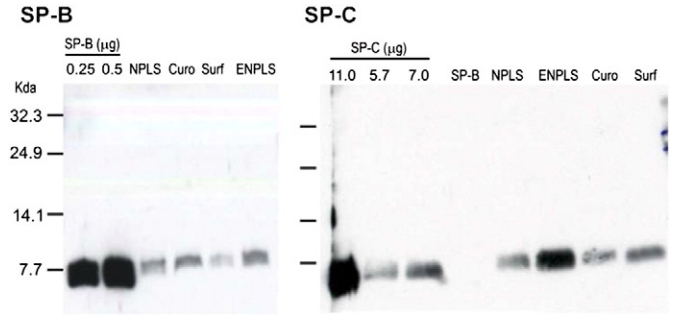

Fig. 2. Analysis of SP-B and SP-C content in Surfacen and native surfactant complexes by Western blot. Western blot analysis using anti-SP-B (left) and anti-SP-C (right) primary antibodies of samples of NPLS, ENPLS and Surfacen (Surf) suspensions. For comparison, an equivalent aliquot of the clinical surfactant Curosurf has been loaded into one lane (Curo), as well as the indicated reference amounts of purified porcine SP-B or SP-C. In the SP-C gel, the lane labelled SP-B was loaded with 2 μg of purified porcine SP-B to illustrate the specificity of the anti-SP-C antibody.

when introduced close to the surface of the air bubble, resulting in equilibrium surface tensions around 23 mN/m within few seconds (Fig. 5a). Post-expansion adsorption was also statistically comparable, indicating that the excess of the three materials could somehow maintain association with the films, so that upon expansion and opening of new interface they could rapidly re-spread and restore the minimal tension. These re-spreading capabilities are confirmed along the quasi-static and dynamic compression–expansion isotherms of the films formed by the three materials (Fig. 5b). Quasi-static cycling showed that NPLS, ENPLS and Surfacen required at least a first compression cycle with a surface area reduction around 34–44% to achieve a minimal surface tension of 2–4 mN/m. During the second compression, only a reduction of around 20% in area is needed for NPLS and ENPLS films to reach the minimum surface tension. The same behavior is achieved from the third cycle by Surfacen films (Fig. 5b, Table 1). The first q-static compression–expansion isotherm was always very different from the fourth one, with markedly larger changes in area and hysteresis, which disappeared in the successive cycles. This could indicate that the three compared materials are efficient in promoting a progressive compression-driven reorganization of the films during the successive compression–expansion cycles. Upon cycling under dynamic regime, at physiologically relevant rates, all the films reached consistently low surface tensions with practically no hysteresis and minimal area reductions below 20% (Fig. 5b, Table 1), while maintaining reduced maximal tensions.

Films formed by NPLS, ENPLS or Surfacen were all highly stable when subjected to mechanical perturbations. Fig. 6 illustrates how films formed by the three materials were able to maintain low tensions $\leq$5 mN/m once the compressed states were subjected to repetitive mechanical perturbations, either after a single quasi-static compression cycle or after 4 q-static and 20 dynamic compression–expansion cycles.

3.3. Structure of surfactant films

Compositional differences between NPLS, ENPLS and Surfacen would anticipate differences in the structure of the different films, in spite of their comparably efficient behavior at the interface. Epifluorescence images of films formed by spreading NPLS, ENPLS or Surfacen aqueous suspensions, doped with 1 mol% of the fluorescent phospholipid probe NBD-PC, at the air–liquid interface and compressed to different surface pressures, are shown in Fig. 7. These images were taken at surface pressures near to the large plateau of the compression isotherm, where maximal segregation of condensed phase domains has been reported [14,15]. The three types of films exhibited segregated dark domains, indicative of the existence of ordered regions with packing excluding the bulky fluorescent probe, but these condensed domains showed very different morphology in the materials compared. Films formed by whole NPLS, segregated under compression conspicuous but very small domains, which reached a maximal size at around 38 mN/m. When the

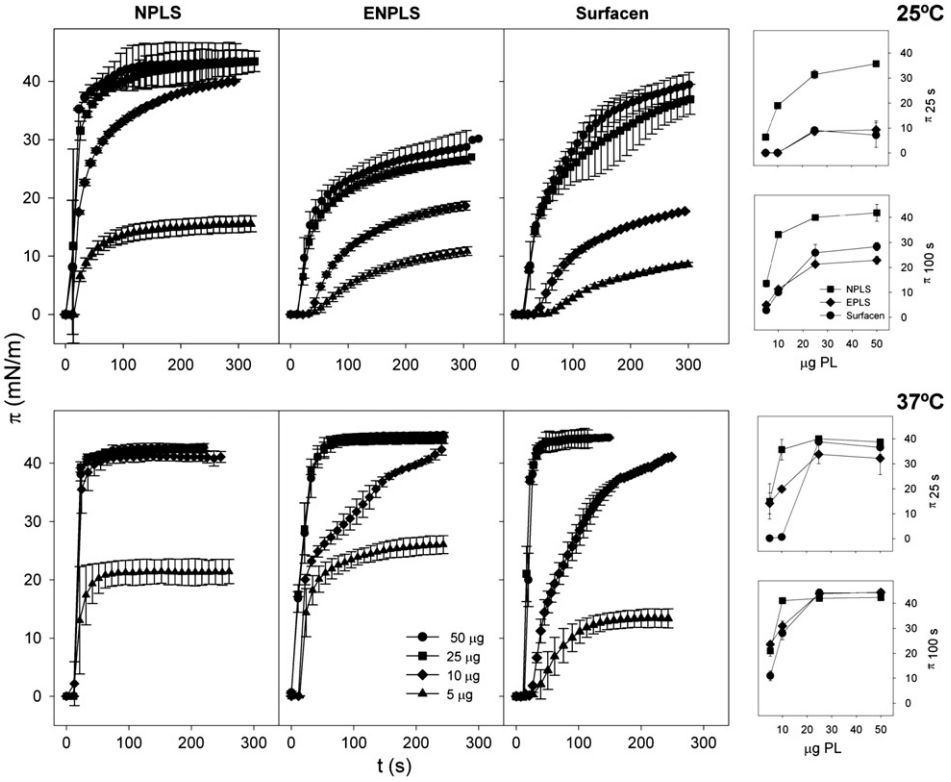

Fig. 3. Interfacial adsorption of Surfacen and native surfactant preparations. π–t isotherms have been obtained upon spreading 5 (▲), 10 (♦), 25 (■) or 50 (●) μg phospholipid of NPLS (left), ENPLS (center) or Surfacen (right) suspensions in a modified Langmuir balance thermostatized either at 25 °C (upper panels) or 37 °C (lower panels). Insets: surface pressure reached by samples at 25 s ($\pi_{25\ s}$) or 100 s ($\pi_{100\ s}$) after applying.

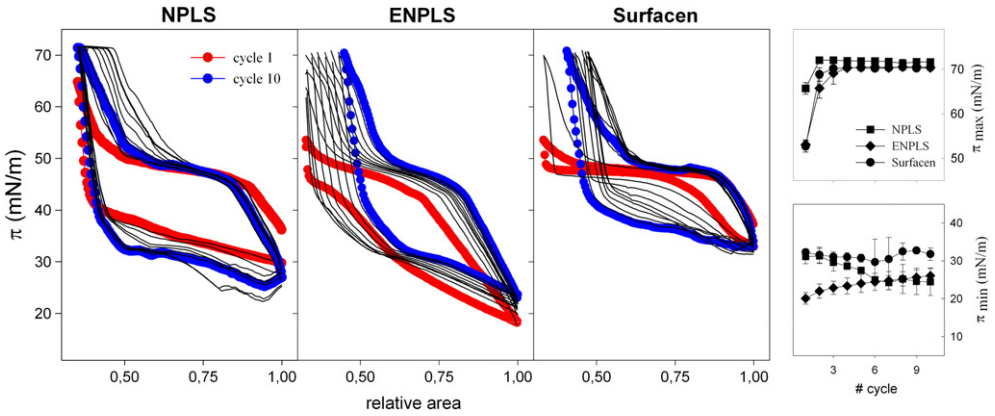

Fig. 4. π–A cycling isotherms of Surfacen and native surfactant films in a Langmuir balance. Ten π–A compression–expansion cycling isotherms have been recorded from NPLS (left), ENPLS (center) or Surfacen (right) films formed by adsorption of the corresponding aqueous suspensions on top of a Tris 5 mM pH 7 subphase containing NaCl 150 mM and thermostatized at 25 °C. Compression rate was 65 cm^2/min. Marked are the first (red) and last (blue) compression–expansion cycle. Insets: maximal (π_{max}) and minimal surface pressure (π_{min}) plotted vs. the number of cycle for NPLS (squares), ENPLS (diamonds) or Surfacen (circles) films.

NPLS films were compressed at pressures higher than that, the size of the domains progressively decreased as well as the apparent contrast between condensed domains and the bright background, so that domains were no longer observed at pressures above the plateau of the isotherm, >45 mN/m. Domains segregated upon compression of films formed by spreading aqueous suspensions of ENPLS were much smaller and markedly less dark than those observed in NPLS films. Domains in ENPLS films seemed also to progressively disappear at pressures above 38–40 mN/m, together with the progressive appearance of bright structures, presumably constituted by three-dimensional surfactant aggregates associated with the interfacial film. In contrast to domains in NSPL or ENPSL films, domains segregated upon compression of Surfacen films showed a high contrast, which was maintained at all the pressures analyzed. Furthermore, Surfacen domains were larger and occupied a larger fraction of area than condensed domains in NPLS or ENPLS. At pressures above 45 mN/m, bright spots of structures presumable protruding in the Z-axis were also present in Surfacen films, although much smaller and more diffusely distributed than those seen in ENPLS layers.

To explore the nature of the marked differences between the lateral structure of compressed ENPLS and Surfacen films, we have analyzed their organization at the submicrometer and nanometer scales by AFM. At large scale, AFM images confirm the presence of more numerous and larger condensed domains in Surfacen films than observed in films formed by ENPLS. Fig. 8 compares illustrative topology and phase AFM images of ENPLS and Surfacen films compressed to 37 mN/m, the surface pressure at which maximal segregation of

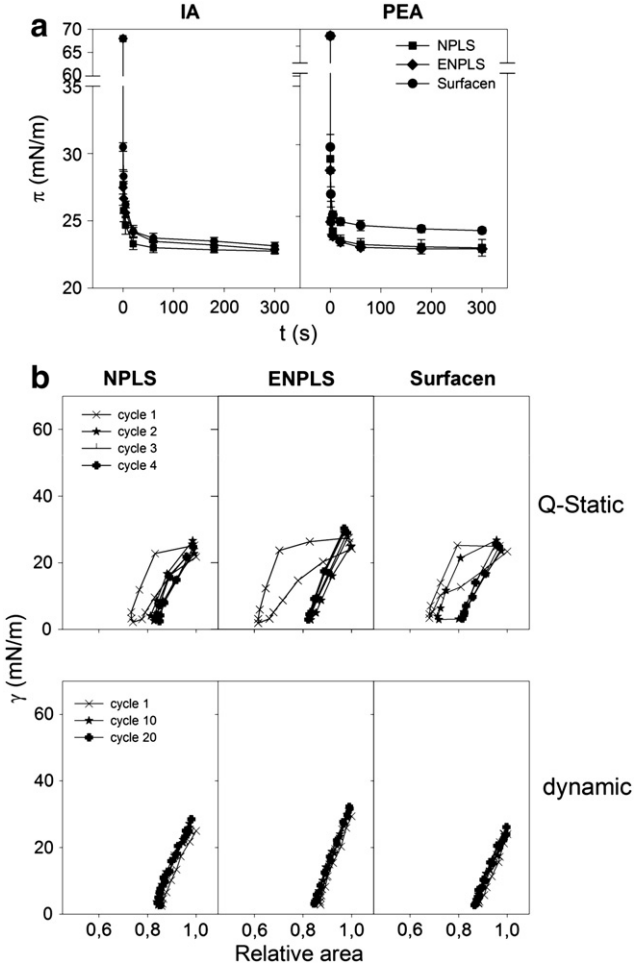

Fig. 5. Surface activity of Surfacen and native surfactant preparations as assessed in the captive bubble surfactometer. (a) Interfacial adsorption of NPLS (squares), ENPLS (diamonds) or Surfacen (circles) suspensions (100 nL, 25 mg/mL) onto the interface of an air bubble in the CBS, thermostatized at 37 °C. Plots compare kinetics upon initial adsorption (IA, left) and after bubble expansion (PEA, right). (b) Quasi-static (upper panels) and dynamic (lower panels) compression–expansion cycling isotherms of bubbles coated with NPLS (left), ENPLS (center) or Surfacen (right) films.

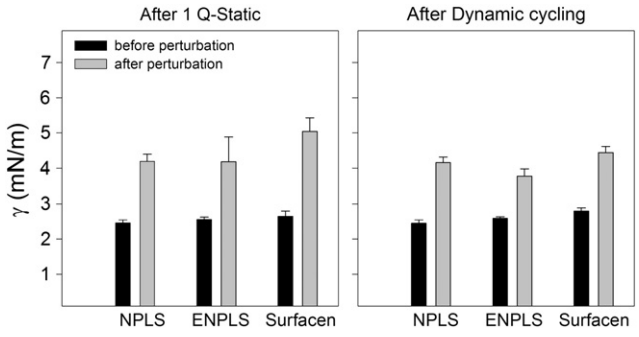

Fig. 6. Stability of compressed Surfacen and native surfactant films against mechanical perturbations. Bars compare minimal surface tension reached by films of NPLS, ENPLS or Surfacen in the captive bubble, before (black bars) and after (grey bars) introduction of 5 consecutive mechanical perturbations discharged on the CBS chamber by a pendulant hammer. Stability of bubbles after one single quasi-static compression cycle (left panel) has been compared with that of bubbles undergoing 4 quasi-static and 20 dynamic compression–expansion cycles (right panel) before introducing the perturbations. Means and standard deviations are shown after averaging 5 different experiments.

Table 1
Parameters defining quasi-static and dynamic compression–expansion isotherms of films formed by NPLS, ENPLS or Surfacen, as assessed in the captive bubble surfactometer.

Surfactant	Quasi-static						Dynamic		
	Cycle 1			Cycle 4			Cycle 20		
	γ_{min}	% Comp.	γ_{max}	γ_{min}	% Comp.	γ_{max}	γ_{min}	% Comp.	γ_{max}
NPLS	2.5 ± 0.31	34.4 ± 6.4	23.9 ± 0.8	2.6 ± 0.6	17.6 ± 2.6	25.8 ± 2.7	2.9 ± 0.57	14.3 ± 2.3	28.4 ± 1.3
ENPLS	2.0 ± 0.17	43.2 ± 6.6	25.7 ± 0.6	2.5 ± 0.6	16.4 ± 2.1	29.5 ± 1.2	2.5 ± 0.7	14.0 ± 2.0	31.9 ± 0.4
Surfacen®	3.4 ± 0.71*,**	34.9 ± 8.3	25.5 ± 1.0*	3.1 ± 0.6	20.9 ± 3.6	27.5 ± 1.5	2.82 ± 0.49	18.3 ± 1.8*	29.6 ± 2.91

γ_{min}: minimum surface tension (mN/m); γ_{max} maximum surface tension (mN/m); % comp.: percentage of compression required to reach γ_{min}.
* Significant difference between NPLS and ENPLS or Surfacen® ($p<0.05$).
** Significant difference between ENPLS and Surfacen® ($p<0.05$).

condensed phase is observed at the microscopic scale. At the largest scale scanned, AFM images show the presence of well-defined micron-size domains, presumably constituted by DPPC-enriched condensed phase, as they show size and distribution that are fully comparable to those of the dark domains observed under epifluorescence microscopy. The higher resolution of AFM shows the clear differences in size and morphology between the segregated domains in Surfacen films and those in ENPLS layers. Domains in Surfacen are larger (diameter 6.8 ± 2 μm) and have a polymorphic flower-like morphology, whilst condensed domains in ENPLS are significantly smaller (diameter 2.3 ± 0.5 μm) and have a much more rounded shape. The expanded phase of both ENPLS and Surfacen, which appeared uniformly bright under the fluorescence microscope, showed a heterogeneous structure at the submicroscopic scale. In the layers of the two materials compared, a percolated matrix of topologically higher, presumably condensed, regions coexists with isolated nanoregions of reduced height, likely consisting of less packed liquid-expanded lipid domains. The contrast between the two types of nanoregions is somehow more evident in the phase-mode AFM images. Interestingly, the difference in height between the two regions in Surfacen (~3 Å) is shorter than that observed in ENPLS films (~7 Å). A detailed observation of the structure of ENPLS and Surfacen films also reveals the presence of higher structures associated with the films. In the ENPLS layers compressed to 37 mN/m one can distinguish the presence of more or less rounded structures of around 100–200 nm of diameter, uniformly distributed at the surface of the films but always on top of regions of higher liquid-condensed phase. These round protruding structures do not almost show contrast in the phase images, where they look comparable to liquid-expanded regions. Such round structures were not practically seen in the Surfacen films. On the other hand, both ENPLS and Surfacen films contained uniformly distributed small clusters of around 30–50 nm, associated almost invariably with liquid-expanded regions and with practically no contrast in the phase images, indicating that they could consist of protruded lipid projections sticking out of the plane of the films. Apart of the differences in the structures protruding out of ENPLS and Surfacen films, the morphology of the two types of layers was entirely comparable with respect to the coexistence of liquid-condensed and liquid-expanded nanoregions and the nanometer scale.

3.4. Thermotropic behavior of surfactant complexes

Fig. 9 summarizes experiments characterizing the thermotropic properties of NPLS, ENPLS and Surfacen complexes, by calorimetry and fluorescence spectroscopy. Membranes of NPLS and ENPLS showed characteristic DSC thermograms (Fig. 9, left panel), similar to those previously published [12,13]. Both types of materials exhibited a broad calorimetric transition, presumably from ordered to disordered lipid phases, associated with an asymmetric endothermic peak, which ends abruptly at temperatures close to 37 °C. Thermogram of Surfacen showed a somehow different morphology, with a less asymmetric peak and more significant contributions at the higher temperature range, above 30 °C. The broad transition of Surfacen ends at temperatures slightly higher, around 39 °C, than those defining the end of transition for NPLS and ENPLS. The enthalpy associated to the transition in Surfacen membranes, 2.6 ± 0.2 Kcal/mol °C, is not significantly different to that associated to the

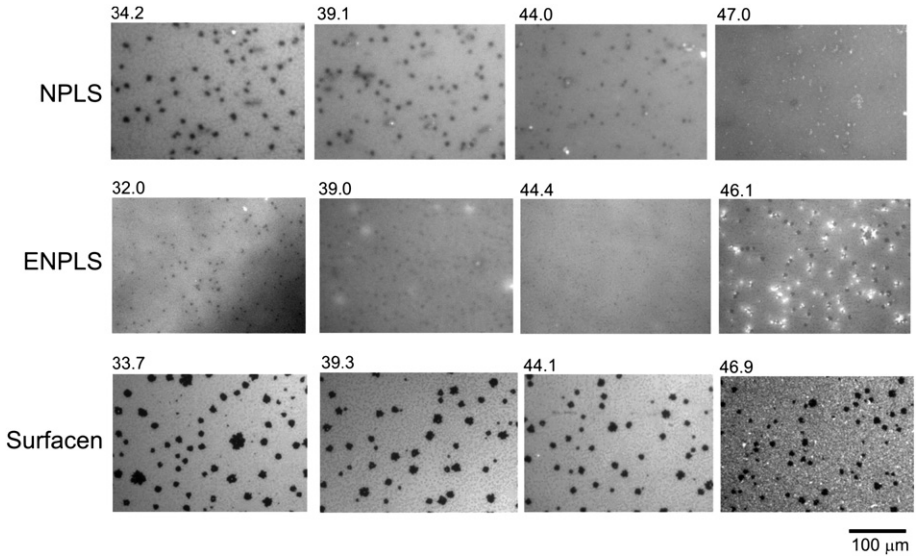

Fig. 7. Structure of Surfacen and native surfactant films as examined by epifluorescence microscopy. Typical images obtained under a fluorescence microscope of NPLS, ENPLS and Surfacen films doped with 1 mol% with respect to phospholipids of NBD-PC, transferred during compression onto glass coverslips using the COVASP technology [31]. Images at the indicated surface pressures were sampled at different positions of the corresponding COVASP film. The films were spread from aqueous suspensions onto the air–liquid interface of a Langmuir surface balance thermostatized at 25 °C, and were compressed at a rate of 25 cm^2/min. All the images have a length of 300 μm.

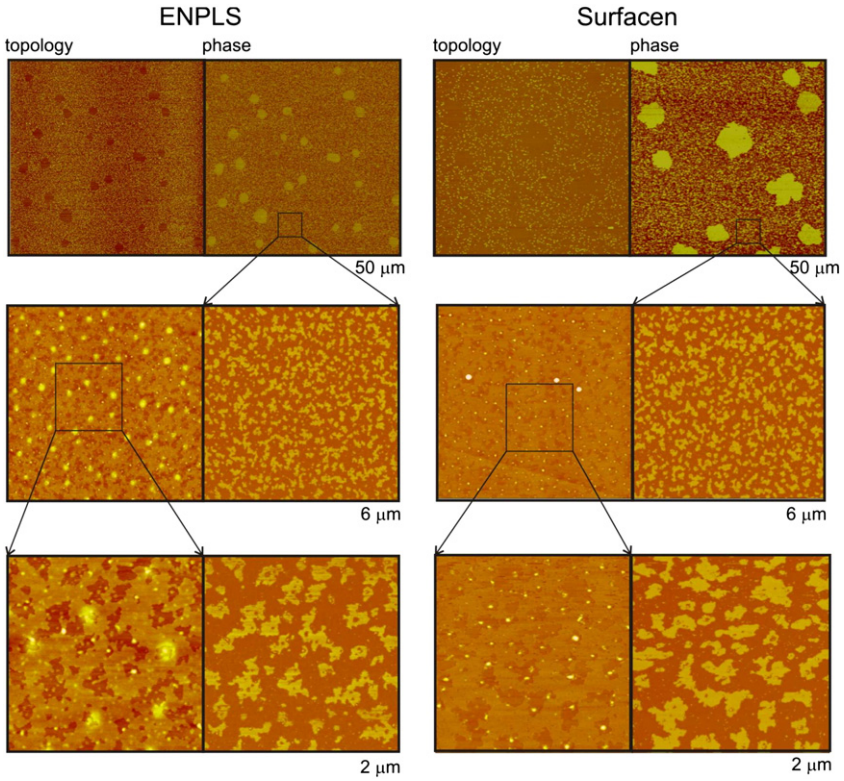

Fig. 8. Structure of Surfacen and native surfactant films as examined by AFM. Typical images obtained by AFM of films formed by spreading organic solutions of ENPLS (left) or Surfacen (right) on a Langmuir surface balance thermostated at 25 °C, compressed at 25 cm^2/min up to 37 mN/m and transferred at constant pressure onto freshly exfoliated mica supports. The figure compares topology images taken under tapping mode (left side of each panel) and images under phase contrast mode (right side of each panel), at three different magnifications covering the lateral distance indicated.

thermotropic transition in ENPLS (2.9 ± 0.4 Kcal/mol °C) or NPLS (2.2 ± 0.1 Kcal/mol °C) samples.

The thermotropic profile of the samples has also been compared analyzing the blue-to-green shift of the emission of a trace of the probe LAURDAN, incorporated into the different complexes. The right panel in Fig. 9 compares the change with temperature of the Generalized Polarization Function of Laurdan (evaluating the spectral shift of the probe emission) integrated in NPLS, ENPLS or Surfacen membranes. These profiles reflect the changes in the microenvironment of the probe when passing from the highly packed dehydrated state of the membranes in the ordered states, at low temperatures, to the more disordered, well-hydrated environment of the probe in membranes in a liquid-disordered state, at temperatures above the phase transition. The three materials compared show indistinguishable Laurdan thermotropic profiles, indicating that temperature-driven transitions in all of them are sensed similarly by a probe that partitions equally in ordered and disordered phases.

4. Discussion

The present study has approached a detailed characterization of the structure and functional properties of Surfacen, a surfactant preparation currently in use to treat neonates at risk of suffering IRDS. This clinical surfactant has contributed to reduce dramatically the mortality of preterm babies in Cuba in the recent years [21,36]. Surfacen is obtained from the organic extract of lipid/protein surfactant complexes pelleted from porcine bronchoalveolar lavage, once subjected to acetone precipitation to reduce the proportion of cholesterol to less than 20-25% of the original content of cholesterol in the source material. Considering the method of production and the lipid and protein composition, Surfacen could be considered a porcine version of BLES, a clinical surfactant obtained from bovine lung lavage, which has been extensively characterized [37–40]. Considering the starting material and the production method of Surfacen and BLES, these natural preparations should contain significant proportions of surfactant proteins SP-B and SP-C, the main protein components responsible for the formation and the dynamic properties of functional surfactant films at the interface [2,29]. We have confirmed that Surfacen contains significant amounts of both SP-B and SP-C, comparable to those accompanying phospholipids in chloroform/methanol surfactant extracts, and also similar to those found in Curosurf, another surfactant preparation of natural origin

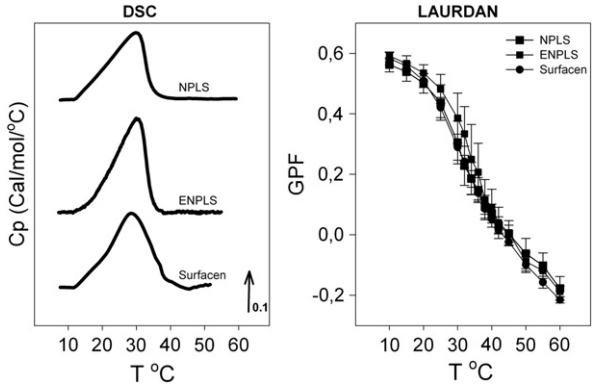

Fig. 9. Thermotropic behavior of Surfacen and native surfactant membranes. Left panel) Typical differential scanning calorimetry thermograms of NPLS, ENPLS and Surfacen suspensions (5 mg/mL phospholipid). Right panel) Thermotropic profile of generalized polarized function (GPF) of the fluorescence of NPLS, ENPLS and Surfacen membranes doped with the probe LAURDAN (1% molar with respect to phospholipids).

obtained from minced porcine lung tissue (see Fig. 2). Acetone precipitation is also widely used to remove protein components from biological samples and there was a possibility that, apart from removing cholesterol, it could also remove some of the protein moiety from the surfactant extracts. We show here that Surfacen still contains a considerable amount of SP-B and SP-C after acetone precipitation, although the absolute proportion of SP-B could be partially reduced compared with material that did not go through acetone treatment (see SP-B bands in the gel of Fig. 2). A main compositional difference of both BLES and Surfacen with respect to their source material, the whole native surfactant and its organic extract, is the significant reduction in cholesterol content. Cholesterol has dramatic effects in the structure, dynamics and surface properties of surfactant. It has been demonstrated that the presence of physiological proportions of cholesterol modulates the lateral segregation of ordered and disordered lipid phases in surfactant membranes [13] and films [41,42], as well as the dynamic behavior of phospholipid species in terms of their diffusion coefficient [12]. On the other hand exacerbated amounts of cholesterol have shown deleterious effects on surfactant interfacial activity [37,39], which motivated the removal of a main fraction of the cholesterol originally present in the natural materials used as a source of practically all the clinical surfactants currently in use [7]. To our knowledge, this is one of very few studies in which the structure and functional properties of a clinical surfactant has been compared in detail with those of the material from which it is derived. The study offers in our opinion a good opportunity to analyze to what extent the procedures involved in the extraction, manipulation and production, storage and distribution of a clinical surfactant preserves the functional properties of the whole native surfactant complexes, and on the other hand, provides complementary information to define the essential features defining a properly active surfactant.

Surfacen and ENPLS suspensions exhibit a significantly slower interfacial adsorption than lipid-protein complexes from full NPLS, which has been usually interpreted in terms of a faster cooperative adsorption of surfactant promoted by protein SP-A [43]. Still, Surfacen shows in the functional tests a very good surface activity, comparable to that exhibited by suspensions of the material extracted from natural surfactant using organic solvents, in terms of i) rapid adsorption to the air–liquid interface (equilibrium surface pressures $\geq$40 mN/m in less than 5 min in the Langmuir trough; surface tensions <25 mN/m in less than 1 min in the CBS), ii) ability to reach very high surface pressures (low surface tensions, <5 mN/m) upon repetitive compression while maintaining high minimal pressures (low maximal tensions, $\leq$30 mN/m) during expansion, and iii) good stability to sustain the lowest tensions (<5 mN/m) upon mechanical perturbation of compressed surface films. Surfacen even exhibits significantly higher minimal surface pressures than native surfactant and its organic extract in films cycled at the Langmuir balance, and a concomitant trend towards lower maximal tensions when cycled in the CBS. The good surface activity of Surfacen is likely related with an appropriate content of hydrophobic surfactant proteins, particularly of SP-B. Enough proportion of SP-B, $\geq$0.4% with respect to phospholipid by mass, has been shown to be essential both to permit surface films reaching the lowest tensions upon minimal area reduction during compression and to sustain minimal tensions even after strong mechanical perturbations [29].

In spite of the remarkable similarity of the interfacial activity of Surfacen with respect to that of films formed by suspensions of porcine surfactant organic extracts, the lateral structure of the films formed by the two materials showed marked differences. Compression originates in Surfacen films the segregation of condensed domains that were significantly larger, more polymorphic and exhibited higher contrast than those observed in ENPLS or NPLS films. This higher contrast is likely related with the relatively higher proportion of DPPC in Surfacen compared with NPLS or ENPLS. The polymorphic flower-like shape of condensed domains in Surfacen can be attributed to the gel-like solid character of DPPC-enriched domains segregated in the absence of cholesterol, as it has been observed in other model systems [44], whilst the more rounded small domains in NPLS and ENPLS likely consist of segregated fluid liquid-ordered phase such as that typical of cholesterol-containing DPPC-enriched regions. Furthermore, condensed domains segregated in Surfacen persisted upon compression of the films up to very high pressures, above 38 mN/m, while virtually disappeared in NPLS or ENPLS films compressed to a similar extent. The remixing of condensed domains in surfactant films compressed beyond threshold pressures has been attributed to the presence of cholesterol [41,42]. Removal of cholesterol in Surfacen could therefore contribute to prevent the structural transformation that occurs in films of natural surfactant compressed up to the so-called squeeze-out plateau, occurring at around 45 mN/m, which molecular nature is still not completely understood. It has been proposed that this level of compression induces a conversion of the condensed micron-sized domains into much smaller nanodomains, whose size prevents observation under the optical microscope [45]. However, the connection between this lateral restructuration and the presence of cholesterol has not been explained yet. The results of the AFM experiments shown here suggest that the removal of cholesterol prevents the formation of certain three-dimensional protrusions, which seem to be originated from the condensed domains in ENPLS films. We propose that in the presence of cholesterol, condensed domains segregated upon compression of full compositionally complex surfactant films actually consist of a fluid liquid-ordered (LO) type of phase. This LO phase could have limited stability at high pressures, leading to partial squeeze-out of material, which could originate a redistribution of fluorescently-labeled components, giving a homogeneous appearance under the low spatial resolution of the epifluorescence images. This could also be the reason why ENPLS films appear as associated with numerous protruded lipid aggregates when analyzed under AFM. It remains to be determined whether protruded structures have a differentiated lipid composition and whether these three-dimensional projections have a thickness consistent with the formation of multilayer stacks. A previous structural study of BLES films, in the absence or presence of physiological proportions of cholesterol, found that cholesterol forms domains within liquid-ordered domains [38]. The present results suggest that segregation of cholesterol-enriched domains within the condensed phase could in fact precede the possible pressure-promoted extrusion of cholesterol-enriched clusters, to end in a cholesterol-depleted film with higher mechanical stability. The observation under AFM of films subjected to more than one cycle of compression revealed the presence of numerous permanently-segregated structures that maintain association with the interfacial film but are highly deformable upon scanning with the AFM tip (not shown). These permanently segregated structures could be the basis of the irreversible depuration/reorganization of surfactant films that occurs during compression, likely related with the progressive loss of hysteresis observed in subsequent compression–expansion cycles at the CBS. Unfortunately, the higher complexity of films subjected to repetitive compression–expansion cycling, including the presence of this highly deformable three-dimensional structures, prevented a more detailed analysis of the processes involved in compression-driven reorganization of surfactant films, which will be the subject of further future studies. In the absence of cholesterol, segregated domains would really consist of a liquid-condensed (LC) solid phase, hardly deformable at high pressures, explaining why Surfacen films lack large protruded lipid aggregates as seen under AFM. The relatively lower solubility of the bulky fluorescent probe into the solid domains of Surfacen would explain their darker appearance with respect to the LO domains in NPLS or ENPLS films. A more efficient segregation of DPPC-enriched ordered LC-like phases could also explain the slight shift of the end of the calorimetric transition in Surfacen membranes towards higher temperatures. The differences in lipid organization and packing could be practically restricted to the local regions where condensed domains nucleate, without producing significant differences in the average hydration state of the different membranes as a whole, according to the information reported by Laurdan.

The differences in morphology between Surfacen and ENPLS films do not seem to be related with detectable important differences in surface activity. Careful examination of the structure of the two types of films at the submicroscopic scale accessible by AFM reveals that once cholesterol has somehow promoted the protrusion into the third dimension of material from ENPLS films, both ENPLS and Surfacen films become constituted by a remarkably similar submicroscopic network of interconnected condensed phase. Exclusion of cholesterol and other possible fluid components from that network is presumably ending in a similarly stable film, able to sustain the maximal pressures without deformation, even upon receiving the shocking waves of dramatic external mechanical perturbations. One could therefore conclude that it is the presence of this fully interconnected condensed network at the nanoscale what defines the adequate rheological properties of surfactant films, required to provide enough stability to the respiratory surface under the demanding conditions imposed by breathing dynamics. A recent study has compared the structure at the nanoscale of films formed by different clinical surfactant preparations [20]. Although the differences found in the structure of these preparations have not been correlated with functional singularities, it is remarkable that an interconnected network of condensed phase similar to that described here was present in the preparations presumably containing the most similar protein compositions to native surfactant.

Production of Surfacen includes lyophilization of surface active lipid–protein suspensions, which are later re-hydrated close to the moment of surfactant administration to babies. The lyophilization process includes a freezing step that, depending on the rate of cooling, could facilitate lipid demixing and phase separation of the mixture of saturated and unsaturated lipid species typically included in Surfacen. Membrane-cooling procedures in the production of Surfacen could induce a particularly efficient segregation of entirely solid DPPC-enriched condensed domains in membranes and films, as observed by epifluorescence microscopy, which could also be behind a more complex calorimetric thermogram, with contributions extended over a wider range of temperatures, compared to that of native surfactant. More solid condensed domains in the interfacial films might be more efficient than relatively fluid LO domains to sustain the highest pressures during compression or to prevent the relaxation of the films during expansion, which could be related with a relatively higher stability of Surfacen films as observed particularly in films compressed at the relatively slow speeds of the Langmuir balance. The situation under breathing conditions in vivo could be different, and it should be determined whether the increase in fluidity and dynamics promoted by cholesterol could have alternative advantages. Additional studies are required to fully characterize the persistence and consequences of the effects of the thermal history experimented by clinical surfactants during their production process, which could be especially relevant to optimize properties such as the stability of the films and their ability to resist environmental perturbations.

Acknowledgements

The authors are particular grateful to Dr. Gemma Fabriàs, Dr. Josefina Casas, and Eva Dalmau, from the Institute of Advanced Chemistry of Catalonia (IQAC-CSIC) (Barcelona, Spain), for their expertise and generous assistance with the compositional analysis of molecular species in the phosphatidylcholine fraction of the surfactant materials. The authors are also grateful to Dr. David Schurch for preliminary experiments of Surfacen in the CBS, to Dr. Barbara Olmeda for her assistance with Western blot analysis, to Dr. Roberto Faure for his continuous scientific support, and to Dr. Mercedes Echaide for her assistance in the preparation of the manuscript. This research has been supported by grants from the Spanish Ministry of Science and Innovation (BIO2009-09694, BFU2010-11538-E, CSD2007-00010, and FIS2009-12964-C05-04), Community of Madrid (S2009MAT-1507 and S2009/PPQ-1642) and the International Cooperation Programmes from the Universidad Complutense and the Agencia Española de Cooperacion y Desarrollo (AECID A/024686/09).

References

[1] C.B. Daniels, S. Orgeig, Pulmonary surfactant: the key to the evolution of air breathing, News Physiol. Sci. 18 (2003) 151–157.
[2] J. Perez-Gil, Structure of pulmonary surfactant membranes and films: the role of proteins and lipid-protein interactions, Biochim. Biophys. Acta 1778 (2008) 1676–1695.
[3] J. Perez-Gil, T.E. Weaver, Pulmonary surfactant pathophysiology: current models and open questions, Physiology (Bethesda) 25 (2010) 132–141.
[4] J.A. Whitsett, S.E. Wert, T.E. Weaver, Alveolar surfactant homeostasis and the pathogenesis of pulmonary disease, Annu. Rev. Med. 61 (2010) 105–119.
[5] T. Fujiwara, H. Maeta, S. Chida, T. Morita, Y. Watabe, T. Abe, Artificial surfactant therapy in hyaline-membrane disease, Lancet 1 (1980) 55–59.
[6] M. Obladen, History of surfactant up to 1980, Biol. Neonate 87 (2005) 308–316.
[7] O. Blanco, J. Perez-Gil, Biochemical and pharmacological differences between preparations of exogenous natural surfactant used to treat Respiratory Distress Syndrome: role of the different components in an efficient pulmonary surfactant, Eur. J. Pharmacol. 568 (2007) 1–15.
[8] B.C. Lam, Y.K. Ng, K.Y. Wong, Randomized trial comparing two natural surfactants (Survanta vs. bLES) for treatment of neonatal respiratory distress syndrome, Pediatr. Pulmonol. 39 (2005) 64–69.
[9] R. Ramanathan, M.R. Rasmussen, D.R. Gerstmann, N. Finer, K. Sekar, A randomized, multicenter masked comparison trial of poractant alfa (Curosurf) versus beractant (Survanta) in the treatment of respiratory distress syndrome in preterm infants, Am. J. Perinatol. 21 (2004) 109–119.
[10] Y.Y. Zuo, R.A. Veldhuizen, A.W. Neumann, N.O. Petersen, F. Possmayer, Current perspectives in pulmonary surfactant—inhibition, enhancement and evaluation, Biochim. Biophys. Acta 1778 (2008) 1947–1977.
[11] I. Mingarro, D. Lukovic, M. Vilar, J. Perez-Gil, Synthetic pulmonary surfactant preparations: new developments and future trends, Curr. Med. Chem. 15 (2008) 393–403.
[12] J. Bernardino de la Serna, G. Oradd, L.A. Bagatolli, A.C. Simonsen, D. Marsh, G. Lindblom, J. Perez-Gil, Segregated phases in pulmonary surfactant membranes do not show coexistence of lipid populations with differentiated dynamic properties, Biophys. J. 97 (2009) 1381–1389.
[13] J. Bernardino de la Serna, J. Perez-Gil, A.C. Simonsen, L.A. Bagatolli, Cholesterol rules: direct observation of the coexistence of two fluid phases in native pulmonary surfactant membranes at physiological temperatures, J. Biol. Chem. 279 (2004) 40715–40722.
[14] B.M. Discher, K.M. Maloney, W.R. Schief Jr., D.W. Grainger, V. Vogel, S.B. Hall, Lateral phase separation in interfacial films of pulmonary surfactant, Biophys. J. 71 (1996) 2583–2590.
[15] K. Nag, J. Perez-Gil, M.L. Ruano, L.A. Worthman, J. Stewart, C. Casals, K.M. Keough, Phase transitions in films of lung surfactant at the air–water interface, Biophys. J. 74 (1998) 2983–2995.
[16] B. Piknova, W.R. Schief, V. Vogel, B.M. Discher, S.B. Hall, Discrepancy between phase behavior of lung surfactant phospholipids and the classical model of surfactant function, Biophys. J. 81 (2001) 2172–2180.
[17] C. Alonso, T. Alig, J. Yoon, F. Bringezu, H. Warriner, J.A. Zasadzinski, More than a monolayer: relating lung surfactant structure and mechanics to composition, Biophys. J. 87 (2004) 4188–4202.
[18] T. Ivanova, I. Minkov, I. Panaiotov, P. Saulnier, J.E. Proust, Dilatational properties and morphology of surface films spread from clinically used lung surfactants, Colloid Polym. Sci. 282 (2004) 1258–1267.
[19] K. Nag, J.S. Pao, R.R. Harbottle, F. Possmayer, N.O. Petersen, L.A. Bagatolli, Segregation of saturated chain lipids in pulmonary surfactant films and bilayers, Biophys. J. 82 (2002) 2041–2051.
[20] H. Zhang, Q. Fan, Y.E. Wang, C.R. Neal, Y.Y. Zuo, Comparative study of clinical pulmonary surfactants using atomic force microscopy, Biochim. Biophys. Acta 1808 (2011) 1832–1842.
[21] O. Moreno V, M. Lee L, F. Domínguez D, et al., Estudio de la eficacia del SURFACEN en el distress respiratorio del recién nacido, Rev. Cuba. Pediatr. 71 (1999) 60–71.
[22] D. Manzanares, E. Díaz, W. Alfonso, A. Escobar, H. Colomé, M.C. Muñoz, M. Noa, S. Rabell, A. Hidalgo, Surfactante pulmonar porcino, Repúb. Cuba A 61 (1995) 35–42 K.
[23] H.W. Taeusch, J. Bernardino de la Serna, J. Perez-Gil, C. Alonso, J.A. Zasadzinski, Inactivation of pulmonary surfactant due to serum-inhibited adsorption and reversal by hydrophilic polymers: experimental, Biophys. J. 89 (2005) 1769–1779.
[24] E.G. Bligh, W.J. Dyer, A rapid method of total lipid extraction and purification, Can. J. Biochem. Physiol. 37 (1959) 911–917.
[25] G. Rouser, A.N. Siakotos, S. Fleischer, Quantitative analysis of phospholipids by thin-layer chromatography and phosphorus analysis of spots, Lipids 1 (1966) 85–86.
[26] D. Canals, D. Mormeneo, G. Fabrias, A. Llebaria, J. Casas, A. Delgado, Synthesis and biological properties of Pachastrissamine (jaspine B) and diastereoisomeric jaspines, Bioorg. Med. Chem. 17 (2009) 235–241.
[27] A. Cruz, J. Perez-Gil, Langmuir films to determine lateral surface pressure on lipid segregation, Methods Mol. Biol. 400 (2007) 439–457.
[28] S. Schurch, F.H. Green, H. Bachofen, Formation and structure of surface films: captive bubble surfactometry, Biochim. Biophys. Acta 1408 (1998) 180–202.

[29] D. Schurch, O.L. Ospina, A. Cruz, J. Perez-Gil, Combined and independent action of proteins SP-B and SP-C in the surface behavior and mechanical stability of pulmonary surfactant films, Biophys. J. 99 (2010) 3290–3299.
[30] W.M. Schoel, S. Schurch, J. Goerke, The captive bubble method for the evaluation of pulmonary surfactant: surface tension, area, and volume calculations, Biochim. Biophys. Acta 1200 (1994) 281–290.
[31] L. Wang, A. Cruz, C.R. Flach, J. Perez-Gil, R. Mendelsohn, Langmuir–Blodgett films formed by continuously varying surface pressure. Characterization by IR spectroscopy and epifluorescence microscopy, Langmuir 23 (2007) 4950–4958.
[32] A. Cruz, L. Vazquez, M. Velez, J. Perez-Gil, Effect of pulmonary surfactant protein SP-B on the micro- and nanostructure of phospholipid films, Biophys. J. 86 (2004) 308–320.
[33] M.V. Picardi, A. Cruz, G. Orellana, J. Perez-Gil, Phospholipid packing and hydration in pulmonary surfactant membranes and films as sensed by LAURDAN, Biochim. Biophys. Acta 1808 (2011) 696–705.
[34] T. Parasassi, G. De Stasio, G. Ravagnan, R.M. Rusch, E. Gratton, Quantitation of lipid phases in phospholipid vesicles by the generalized polarization of Laurdan fluorescence, Biophys. J. 60 (1991) 179–189.
[35] C.J. Pynn, M.V. Picardi, T. Nicholson, D. Wistuba, C.F. Poets, E. Schleicher, J. Perez-Gil, W. Bernhard, Myristate is selectively incorporated into surfactant and decreases dipalmitoylphosphatidylcholine without functional impairment, Am. J. Physiol. Regul. Integr. Comp. Physiol. 299 (2010) R1306–R1316.
[36] O.N.d.E.e, Información, Cuba: Proyección de la Población; Nivel Nacional y Provincial, Periodo 2010–2011, In: Anuarios Demográficos de Cuba, Oficina Nacional de Estadísticas e Información, 2010.
[37] L. Gunasekara, S. Schurch, W.M. Schoel, K. Nag, Z. Leonenko, M. Haufs, M. Amrein, Pulmonary surfactant function is abolished by an elevated proportion of cholesterol, Biochim. Biophys. Acta 1737 (2005) 27–35.
[38] E. Keating, L. Rahman, J. Francis, A. Petersen, F. Possmayer, R. Veldhuizen, N.O. Petersen, Effect of cholesterol on the biophysical and physiological properties of a clinical pulmonary surfactant, Biophys. J. 93 (2007) 1391–1401.
[39] Z. Leonenko, S. Gill, S. Baoukina, L. Monticelli, J. Doehner, L. Gunasekara, F. Felderer, M. Rodenstein, L.M. Eng, M. Amrein, An elevated level of cholesterol impairs self-assembly of pulmonary surfactant into a functional film, Biophys. J. 93 (2007) 674–683.
[40] Y.Y. Zuo, S.M. Tadayyon, E. Keating, L. Zhao, R.A. Veldhuizen, N.O. Petersen, M.W. Amrein, F. Possmayer, Atomic force microscopy studies of functional and dysfunctional pulmonary surfactant films, II: albumin-inhibited pulmonary surfactant films and the effect of SP-A, Biophys. J. 95 (2008) 2779–2791.
[41] B.M. Discher, K.M. Maloney, D.W. Grainger, S.B. Hall, Effect of neutral lipids on coexisting phases in monolayers of pulmonary surfactant, Biophys. Chem. 101–102 (2002) 333–345.
[42] B.M. Discher, K.M. Maloney, D.W. Grainger, C.A. Sousa, S.B. Hall, Neutral lipids induce critical behavior in interfacial monolayers of pulmonary surfactant, Biochemistry 38 (1999) 374–383.
[43] S. Schurch, F. Possmayer, S. Cheng, A.M. Cockshutt, Pulmonary SP-A enhances adsorption and appears to induce surface sorting of lipid extract surfactant, Am. J. Physiol. 263 (1992) L210–L218.
[44] L.A. Bagatolli, E. Gratton, Two photon fluorescence microscopy of coexisting lipid domains in giant unilamellar vesicles of binary phospholipid mixtures, Biophys. J. 78 (2000) 290–305.
[45] Y.Y. Zuo, E. Keating, L. Zhao, S.M. Tadayyon, R.A. Veldhuizen, N.O. Petersen, F. Possmayer, Atomic force microscopy studies of functional and dysfunctional pulmonary surfactant films. I. Micro- and nanostructures of functional pulmonary surfactant films and the effect of SP-A, Biophys. J. 94 (2008) 3549–3564.